Benchmarking approach for empirical comparison of pricing models in DRMS

Seif Azghandi, Kenneth Mark Hopkinson, Kennard Robert Laviers

Department of Electrical and Computer Engineering, Air Force Institute of Technology, 2950 Hobson Way, Wright-Patterson AFB, OH 45433, USA
E-mail: seifullah.azghandi@afit.edu

Published in *The Journal of Engineering*; Received on 1st August 2016; Accepted on 26th September 2016

Abstract: Demand response management systems often involve the use of pricing schemes to motivate the efficient use of electrical power. Achieving this efficiency requires the detection of electrical power patterns. The detection of these patterns normally involves use of non-linear, quasi-non-linear, and at times linear data pattern detection models. The behavioural disparities of these models and specifically when used for a specific set of data make it hard to select the most efficient model. The contribution of this study is devising an empirical benchmark (reference) (*perfect*) control pricing (PCP) model through which various models are compared in order to select the most efficient model. In this study, the authors elect neural networks, sliding window–multiple linear regression, and a proportional controller models to be representative of non-linear, quasi-non-linear, and linear models, respectively, in order to demonstrate the effectiveness of PCP. The dataset used for demonstrating both the operation of PCP and the elected models for comparisons is collected from Green Button project and Pacific Gas and Electric.

1 Introduction

At the heart of the demand response management system (DRMS) is a pricing scheme whose goal is often, at least in part, intended to motivate the efficient use of electrical power. A key idea in this type of approach is to discourage unnecessary use of electrical power during peak usage hours via higher pricing. From the consumer's perspective (demand side), the incentive is to receive a lower electrical power usage bill. From the utility company's perspective (response side), the incentive is to avoid the cost of building additional generators and preventing potential blackouts that can result from excess electrical power usage. The assumption is that an appropriate pricing scheme discourages unwise electrical power consumption and consequently acts as a regulating mechanism for prudent electrical power usage. For a utility company serving a geographical area, the goal is to compute the maximum electrical power delivery capability for that geographical area, and set a usage threshold to avoid getting close to that limit. A pricing scheme can then be created that penalises the consumer through higher electrical power consumption costs when the regional electrical power usage rises over a pre-determined threshold during peak demand hours. This pricing scheme should keep the electrical power consumption level under the set usage threshold and rarely, if ever, exceed the maximum electrical power delivery capacity. In this paper's experiments, the goal of the control system is to keep electrical power usage *hovering around* the set usage threshold, but a utility may choose to keep the set usage at or below the set usage threshold instead using the same basic methods. Given the task above, we formulate the following problem statement: given an electrical power usage tolerance range determined by a utility company, the amount of electrical power consumed, and considering an estimate of the consumers' price elasticities [1], we must devise a pricing scheme that discourages the excess use of electrical power during peak time periods. To craft a solution to this problem, the power utility companies must be able to detect electrical power usage patterns in specific geographical areas and be able to estimate a population's price response. Both are required to calculate appropriate price points to match specific circumstances. There are notable challenges in achieving this goal. A power utility company could be serving the needs of single/multiple families, small/medium/large businesses, municipalities/schools, spread across various regions. These regions might consist of diverse settings and populations include mountainous, coasts, deserts, and urban/rural areas. Utility electrical power consumption datasets may contain anomalies such as abnormal use during holiday seasons, and may require some preprocessing before they can be analysed and used as the basis for usage pattern analysis. The efficiency, both in terms of computation and accuracy, by which the consumed electrical power data is processed has an impact on the result. Additional processing and trend analysis is also typically performed to predict consumer's reactions to price fluctuations. For the remainder of this paper, we will refer to electrical power as power for brevity purposes. In this paper, we propose to use a benchmark (reference) model called (*perfect*) control price (PCP) through which the selection of the most suitable model is achieved by comparing each and every model against PCP. There are two advantages for using PCP. First, in absence of PCP, there would be $[n(n-1)]/2$ pairwise (in quadratic time) comparisons among the models, whereas comparing PCP against each and every model results to n (in linear time) comparisons. Second, use of a PCP becomes imperative when disparities among the models prevent direct comparisons. Using PCP, the selection of the best model under comparison amounts to selection of the difference (delta) with the lowest value (i.e. closest to PCP) and/or considering other tradeoffs such as complexities, level of accuracy etc. The general construction of PCP model is by using the publicly available power consumption dataset obtained from the *Green Button* project and Pacific Gas and Electric (PG&E) [2]; the dataset, then, is processed to fit a 1 year case study period and interpolation/extrapolation is used to represent the data in 15 min intervals. Next, simulating consumer's *adjusted* elasticity (EL_{ij}), we compute a unit price [per kilowatts (KW)] such that the *arithmetic product* of the consumed power and the computed unit price *equates* that of *arithmetic product* of preset (threshold) power and the *base* unit price for each and every 15 min interval throughout the year. That is, the arithmetic product of consumed power and unit price (considering elasticity) computes to be *constant* for each and every 15 min interval since the computed and fluctuated unit price *controls* or *regulates* the amount of power to consume. Note, that initial values of elasticities per customer type ($\mathrm{EL}_{\mathrm{CT}}$) are set either through the home's *intelligent* centralised controller unit that automatically selects the most efficient elasticity based on consumed power patterns or the consumer selects it manually. In our simulation, the initial values of elasticities per customer type ($\mathrm{EL}_{\mathrm{CT}}$) are selected arbitrarily for simulation purposes. However, irrespective of elasticity selection or generation method, the product of unit price and the consumed power computes to be identical for each and every 15 min interval. To demonstrate the utility of PCP in selecting the most efficient pricing model, we elect neural networks (NNs), sliding windows–multiple linear regression (SWMLRs), and proportional controller (PCntlr) to *represent* non-linear, quasi-non-linear, and linear models, respectively. The justification for selections of these models are that NNs represent non-linear behaviour (scalable through adding additional *hidden* layers) and its practical use is accommodated by various powerful software tools such as MATLAB; the SWMLR simulates quasi-non-linear behaviour through orchestration of *piecewise* linear models to simulate non-linearity and PCntlr exhibits simplistic linear behaviour in a relatively inaccurate form. Hence, the use of the three representative models delineates their degree of accuracy relative to PCP for comparison purposes. Fig. 1 depicts a model of the paper's DR test system. This figure demonstrates that a pricing model controls (regulates) the consumer power system through a negative feedback loop to compute the new demand. The rest of this paper is organised as follows. Section 2 reviews related literature. Section 3 describes and formalises the (post-processed) PCP including its construction and a sample data followed by formalisation of NNs, SWMLR, and PCntlr. Section 4 explains the case study data, the preprocessing performed, and the basic assumptions made. Section 5 describes and analyses the results of the comparisons (differences or deltas) produced from running the foregoing models on the preprocessed data in the paper's case study. Section 6 concludes the paper.

2 Related work

This section summarises related work involving DRMs using a variety of approaches. Ozturk *et al.* [3] proposed a load forecasting and appliance scheduling time of use scheme. The authors used an adaptive neural fuzzy inference system in which the NN component was responsible for learning the system and used fuzzification to compensate for inaccuracies. Samadi *et al.* [4] suggested a real-time pricing algorithm that used message interchanges between energy consumers and utilities in order to relay real-time price (RTP) information. This work was conducted by utilising energy consumer preferences/usage patterns employing utility functions based on microeconomics principles. Roos and Lane [5] presented an RTP scheme considering an installed plant's power generation capabilities, the plant's spare energy capabilities, and the structure of the RTP tariff. Aalami *et al.* [6] proposed demand side management (DSM) based on time of use and an emergency DR programme by using single- and multi-period load models via a load elasticity concept. Su and Kirschen [7] quantified demand–respond effects on electricity markets through a centralised complex-bid market-clearing approach. Xie *et al.* [8] addressed the supply and demand RTP problem by considering the use of wind and solar power. The authors used look-ahead model-predictive (Markov) control. Goel *et al.* [1] introduced a spot pricing scheme that interacted mutually with loads. The interaction used a self-/cross-elasticity matrix. The effects on nodal prices were investigated using optimal power flow techniques. Li *et al.* [9] proposed DSM considering household appliances including plug-in hybrid electric vehicles and batteries based on utility maximisation. The authors claim that individual optimality could be aligned with social optimality. Keogh *et al.* [10] indicated the use of SWMLR as an approach for piecewise linear approximation in time-series datasets. The preceding works indicate the theoretical treatment of DRMS, and therefore the justification of our approach in treating the DRMS in an empirical fashion. Furthermore, the contribution of this paper is in devising a PCP model that serves as a benchmark to facilitate the comparisons of the candidate pricing models through numerical methods where theoretical model comparisons are unwieldy.

3 PCP model

The PCP model for power is best described by the following statement: given a weight-adjusted consumed power for a geographical area – *raw overall* (**RO**), a fluctuating (computed) unit price (**rp**) representing increased/decreased unit price based on demand for power and elasticity (***EL***) in a time interval, devise a pricing scheme that discourages (minimises) the excess power demand. Note that we need a set of initial conditions of *base price* ($\mathrm{rp_b}$), *base RO* ($\mathrm{RO_b}$) to establish the various threshold values before proceeding with the rest of the 15 min intervals' computations. We formalise this goal with the following objective function:

$$\underset{f}{\operatorname{argmin}} \parallel \mathbf{RO},\ \mathbf{rp},\ \boldsymbol{EL}) \parallel = \boldsymbol{K}, \tag{1}$$

where $\mathbf{RO} = \{\mathrm{RO}_1,\ \mathrm{RO}_2,\ \ldots,\ \mathrm{RO}_n\}$ represents the total weighted consumed power for all consumer types ($\mathbf{CT} = \{\mathrm{CT}_1,\ \mathrm{CT}_2,\ \ldots,\ \mathrm{CT}_D\}$) in each 15 min time interval for a full year (n represents the number of total weighted consumed power for a full year), $\mathbf{rp} = \{\mathrm{rp}_1,\ \mathrm{rp}_2,\ \ldots,\ \mathrm{rp}_n\}$ is the *random price*, ***EL*** ($\mathrm{EL}_{ij} \in \boldsymbol{EL}$) is an $\{n \times D\}$ vector ($\mathrm{EL}_{11},\ \ldots,\ \mathrm{EL}_{Dn}$) with its members paired up with those of consumed power for a given customer type in 15 min time interval; i.e. ($\{\mathrm{CT}_1,\ \mathrm{EL}_{\mathrm{CT}_1}\},\ \{\mathrm{CT}_2,\ \mathrm{EL}_{\mathrm{CT}_2}\},\ \ldots,\ \{\mathrm{CT}_D,\ \mathrm{EL}_{\mathrm{CT}_D}\}$). The word *random*, in rp, is used from the consumer's perspective since a consumer is not privy to the justification for price fluctuations enforced by the utility company.

The elasticities for all the customer types, $\mathrm{EL_{CT}}$, are determined and set to a normalised ratio in the range of 0 and 1 ($0 \simeq< \mathrm{EL_{CT}} \le 1$); $\mathrm{EL_{CT}} = 1$ implies that a particular CT is completely willing (*elastic*) to adjust the power usage according to utility company price changes, and $\mathrm{EL_{CT}} \simeq 0$ implies unwillingness of a particular consumer (completely *inelastic*) to adjust the power usage regardless of price changes. Utility companies can estimate customer type elasticity values using historical power data and past consumer behaviour or a customer could select it using their centralised controller unit. Section 3.1 demonstrates how customer type elasticity, $\mathrm{EL_{CT}}$ values are *adjusted* to elasticity values (EL_{ij}), using the fluctuated price. $\mathbf{K}(K_1 = K_2 = K_3 = \cdots = K_n)$ is the numerical value representation for (perfect) *control demand* (**PCD**) consumed power that *computes to be unchanging* (constant)

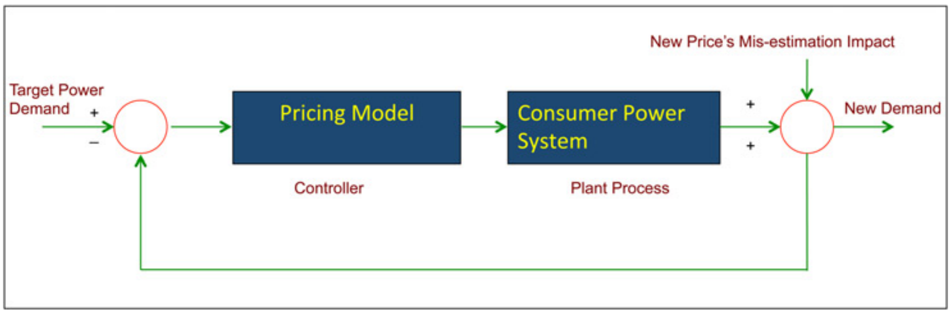

Fig. 1 *Model of the power DR test environment used in this paper*

Table 1 PCP sample computed data

RO, MW	OE	IM, MW	ND, MW	PCP, cents	PCD, MW
291563.6	0.00	0.00	291563.6	0.10	291563.6
271848.4	0.00	0.00	271848.4	0.11	291563.6
269298.4	−0.36	−96473.30	172825.14	0.17	291563.6
279600.9	−3.39	−948902.80	−669301.96	−0.04	291563.6

despite the fluctuations in a given random price (rp_i) for *any* given 15 min collected consumed power interval.

3.1 Construction of PCP model

The construction of the PCP model starts by summing over the weighted ($W_i = \{W_1, \ldots, W_D\}$) consumed power for CTs ($\mathrm{CT}_i = \{\mathrm{CT}_1, \ldots, \mathrm{CT}_D\}$) per time interval (i.e. 15 min) for a geographical area (RO – RO_i)

$$\mathrm{RO}_i = \sum_{j=1}^{D} W_{ij} \cdot \mathrm{CT}_{ij}, \tag{2}$$

where D is the number of different CTs [e.g. single-family (SF), multi-family (MF) etc.], W_{ij} is the (unit-less) weight of the consumed power for a given CT (CT_{ij}) in the time-interval relative to its corresponding RO (RO_i); i.e. $W_{ij} = \mathrm{CT}_{ij}/\mathrm{RO}_i$, where $\sum_{j=1}^{D} W_{ij} = 1$. PCP model also takes into account the temperature readings associated with each and every CT as part of its dataset; however, temperature is used as an *explanatory* variable in NNs and SWMLR models and is not utilised in construction of PCP benchmark model

$$T_i = \sum_{j=1}^{D} W_{ij} \cdot T_{ij}, \tag{3}$$

where $T_{ij} \in \mathbf{T}$ is the temperature reading for a given CT in a given time interval. These temperature readings are used as a parameter in NNs and SWMLR to estimate unit price. Assuming a preset (pre-agreed) *base price*, $\mathrm{rp_b}$ (e.g. 10 cents per kW) for consumed power at threshold level, we define elasticity, EL_{ij}, by 4. EL_{ij} is unit-less *price-adjusted* elasticity for a given customer type

$$\mathrm{EL}_{ij} = \frac{\mathrm{PCP}_i - \mathrm{rp_b}}{\mathrm{rp_b} \cdot \mathrm{EL}_{\mathrm{CT}_j}}, \tag{4}$$

where $\mathrm{EL}_{\mathrm{CT}_j} \neq 0$, $\mathrm{PCP}_i = \mathrm{rp_b}$ for $i = 1$, and $\mathrm{PCP}_i = \mathrm{PCP}_{i-1}$, for $i \geq 2$. We define (unit-less) *overall elasticity*, OE_i, for *all* the customer types (in a 15 min time interval) as the weighted sum of EL_{ij}'s

$$\mathrm{OE}_i = \sum_{j=1}^{D} \mathrm{EL}_{ij} \cdot W_{ij}, \tag{5}$$

Subsequently, *impact* (IM_i) of OE (OE_i) for RO (RO_i), measured in megawatts (MW) and a 15 minute time interval, is defined as

$$\mathrm{IM}_i = \mathrm{RO}_i \cdot \mathrm{OE}_i, \tag{6}$$

and net demand (ND_i), measured in MW for a 15 min time interval, is defined as

$$\mathrm{ND}_i = \mathrm{RO}_i + \mathrm{IM}_i, \tag{7}$$

Considering (2)–(7), PCP (PCP_i) for a 15 min time interval is defined as

$$\mathrm{PCP}_i = \mathrm{rp_b} \cdot (\mathrm{RO_b} - \mathrm{ND}_i) + \mathrm{PCP}_{i-1}, \; i \geq 2 \tag{8}$$

Note that for $i = 1$, $\mathrm{ND}_i = \mathrm{RO_b}$ and $\mathrm{PCP}_i = \mathrm{rp_b}$ and the PCD (PCD_i) for a 15 min time interval is defined as

$$\mathrm{PCD}_i = \mathrm{ND}_i \cdot \frac{\mathrm{PCP}_i}{\mathrm{rp_b}}, \; i = 1 \tag{9}$$

where $\mathrm{PCD}_i = K_i$ (*constant value*) is alluded to in Section 3 and $\mathrm{RO_b}$ is the preset threshold power usage at which base price ($\mathrm{rp_b}$) is set. Equations (4)–(8) act as the regulating mechanism (alluded to in Section 1) that keeps the power consumption at the preset threshold level. Note that the categorisation of total consumed power per time interval (RO_i) into various regions and customer types has no effect on the price (PCP_i) computation.

3.2 PCP sample computed data

Table 1 contains sample computed data for the principal parameters (intermediary parameters are skipped due to space limitation) illustrating the construction of PCP (Section 3.1). Referring to Table 1, the top data row establishes the base line ($\mathrm{rp_b} = 0.10$, with $\mathrm{ND}_i = 291563.60$) with the succeeding row of data representing randomly selected computed data. As demonstrated, the column, PCD_i computes to be constant due to computations in column PCP_i.

3.3 PCntlr model

A PCntlr is a linear feedback control system in which the feedback value helps in adjusting for the potential perturbation in order to keep the system in a stable (preset) condition. This paper adopts a PCntlr formulation based on work from Minorsky [11] and Liptak [12]. Formally, the PCntlr can be defined as

$$P_{\mathrm{out}} = K_{\mathrm{p}} \cdot (\mathrm{SP} - \mathrm{PV}) + P_0 \tag{10}$$

where P_{out} is the output of the PCntlr, K_{p} is the proportional gain, SP is the set point, PV is the process variable, and P_0 is the controller's output with no error. The term (SP – PV) is the instantaneous error [$E(t)$]. The PCntlr price is derived in an analogous way to (8) and (9) in Section 3 (and units) for a 15 min interval

$$\mathrm{PCntlr\_price}_i = \mathrm{rp_b} \cdot (\mathrm{ND}_i - \mathrm{RO_b}) \tag{11}$$

and the $\mathrm{PCntlr\_demand}_i$ is defined as

$$\mathrm{PCntlr\_demand}_i = \frac{\mathrm{PCntlr\_price}_i}{\mathrm{rp_b}} \tag{12}$$

3.4 NNs model

NNs can be described by the mapping, through non-linear functions, a set of input variables $\boldsymbol{X}$ to a set of output variables $\boldsymbol{Y}$ controlled by sets of adjustable weight parameters, $\boldsymbol{W}$ [13]. NNs use *back-propagation*, among the other techniques, to *learn* a model of the system. One of the drawbacks of NNs is the learning time overhead. In this paper, we have elected to use two-layer feed-forward NNs

$$y_k(\mathbf{X}, \mathbf{W}) = \sigma\left(\sum_{j=1}^{M} w_{kj}^{(2)} h\left(\sum_{i=1}^{D} w_{ji}^{(1)} x_i + w_{j0}^{(1)}\right) + w_{k0}^{(2)}\right) \tag{13}$$

where the superscripts (1) and (2) denote the weights in their respective layers, $h(\sum_{i=1}^{D} w_{ji}^{(1)} x_i + w_{j0}^{(1)})$ is the *activation* function, and $w_{j0}^{(1)}$ is the jth intercept weight for M hidden units in layer 1 (corollary, $w_{k0}^{(2)}$ is the kth intercept weight for M hidden units in layer 2). In NNs, selecting a large or small number of hidden units results to over-fitting or under-fitting, respectively. However, the *optimal* number of hidden units is dependent on the data distribution and varies for different datasets. This is the main contributing factor leading to NNs' complexity. *Gradient descent* is an optimisation technique that modifies the weights of the connections leading to hidden units in such a way that minimises the difference between the desired output and the current output, commonly referred to as the *error function*; error minimisation normally occurs over many iterations. Assuming x as an input vector comprised of values (a) and their associated weights (w), $f(x)$ as an output function, and y as an output value, we would like to minimise the error function (E) with respect to the associated weights [14]. Equation (14) formulates a simplified NN with a hidden layer in which $f(x)$ represents a sigmoid function $[1/(1+\mathrm{e}^{-x})]$

$$\frac{\mathrm{d}E}{\mathrm{d}w_{ij}} = \big(f(x) - y\big) f'(x) w_i f'(x_i) a_j \tag{14}$$

Equation (14) calculates a change of a particular weight (w_{ij}) with respect to a particular input value (a_j). For each training instance, a

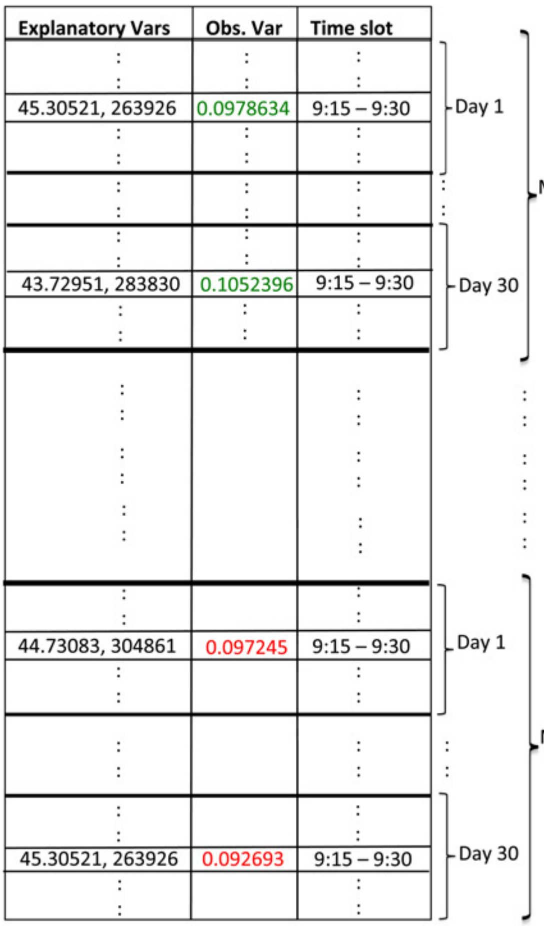

Fig. 2 *'Month 1' is the training set where the fitting models are built. The remaining months are the testing sets where the predicted unit prices are computed. The training set is made of 30 days with each day consisted of 24 h of 15 min time intervals 96 (4 × 24) corresponding to 96 fitting models. The unit prices in green text (i.e. the middle columns in days 1..30 in Month 1) are indicative of training sets instrumental in building the fitting models. The fitting models are used to impute the predicted unit prices in the testing set for the corresponding time intervals. The unit prices in red text (i.e. the middle column in Month 12 in days 1..30) are imputed predictive unit prices for the testing sets*

summation is calculated over the changes for w_{ij}, the result is multiplied by the *learning rate* [current output value/targeted output value ≤ 1.0], and this result is subtracted from the current w_{ij} value.

3.5 SWMLR model

The behavioural operation of SWMLR model consists of two interacting behaviours. The first is the use of a SW and the second is the application of MLR. The MLR's goal is to *fit* a linear line (also called *fitting model*) for the given dataset by establishing a relationship between multiple *explanatory* (independent) variables and *response* (also called *observed*) variables. The goal of the sliding the window (SW) is to update the MLR for the specific segment of the dataset. Using this scheme, the dataset will be *piecewise* collection of linear models with various slopes; the collection of slopped lines depicts the non-linearity of dataset. This is also referred to as piecewise linear approximation [10]. The use of SW may result in a representation of the non-linear behaviour (quasi-non-linear model) of the datasets depending on the number of fitting models used. The general form of MLR is $\mathbf{y} = \mathbf{X}\boldsymbol{\beta} + \boldsymbol{\varepsilon}$ in which $\mathbf{y}$ is a set of *predicted* responses, $\mathbf{X}$ is a set of explanatory variables, $\boldsymbol{\beta}$ is a set of coefficients for explanatory variables (including the intercept – $\boldsymbol{\beta}_0$), and $\boldsymbol{\varepsilon}$ is the set of residuals. For the ith iteration, the preceding equation takes the following form: $y_i = \beta_1 x_{i1} + \cdots + \beta_p x_{ip} + \varepsilon_i = \mathbf{x}_i^{\mathrm{T}}\boldsymbol{\beta} + \varepsilon_i,\ i = 1, \ldots, n$. $\boldsymbol{\beta}$ is calculated by $\boldsymbol{\beta} = (\mathbf{X}^{\mathrm{T}}\mathbf{X})^{-1}\mathbf{X}^{\mathrm{T}}\mathbf{y}$, where $\boldsymbol{X}$ is the vector of explanatory variables, $\mathbf{X}^{\mathrm{T}}$ is the transposition of $\boldsymbol{X}$, $(\mathbf{X}^{\mathrm{T}}\mathbf{X})^{-1}$ is the inverse, and $\boldsymbol{y}$ is the vector of observed values.

3.5.1 SWMLR data structure: Referring to Fig. 2, SWMLRs data structure in our experiment consists of a *training* portion, which is instrumental in generating the models, and the *testing* portion, which is used for comparison against PCP. The training portion of SWMLR consists of a set of data points for 1 month (30 days). Each day of data is further broken down into 96 (4 × 24) 15 min time-interval datasets; each dataset in the training portion contains values for two explanatory variables. Namely, the dataset consists of a *temperature RO* (T_RO) value, a RO value, and a value for an observed variable representing the unit price (unit_price). The observed unit price values are obtained from the first month's PCntlr's computed unit price values in order to bootstrap the SWMLR system. This is done because PCntlr does not require historical prices/training sets to operate, but SWMLR does. After the first month of data, SWMLR operates independently of PCntlr going forward. In Fig. 2, the observed values in the training portion are shown in green text (i.e. the middle column in Month 1 for days 1..30). The testing portion of data structure replicates the structure of the training portion with the exception of unit price. The testing portion consists of 11 months. The fitting models use imputation to predict missing unit price values. In Fig. 2, the testing portion's predicted unit price values are shown in red text (i.e. the middle column in days 1..30 in Month 12).

3.5.2 SWMLR's processing: The goal of SWMLR processing is to impute (i.e. predict) the missing future unit prices in the test portion by (i) constructing a fitting model (see Section 3.5) for each time slot in the training portion and (ii) applying each constructed model to its corresponding time-slot independent variables in the testing portions. Iterating through the preceding steps 1 and 2, the predicted unit price values are imputed in a sparse manner until all (96) fitting models are applied. This effectively fills out the entire testing portion's unit prices with the predicted values. The last steps boost the data by randomly selecting six chunks of data from the newly constructed SWMLR data structure and averaging them to be used against PCP.

Table 2 Power distribution in buses 5, 6, and 8

Bus number	SFs (20%), MW	MFs (40%), MW	Biz. (20%), MW	Agr. (20%), MW
5 (270 MW)	54	108	54	54
6 (350 MW)	70	140	70	70
8 (220 MW)	44	88	44	44

Table 3 Sample data demonstrating increase/decrease in consumed power and unit price

Consumed power in %wrt total consumed power per CT in all four regions	Preset threshold (RO_b), MW	5% inc. wrt RO_b, MW	5% dec. wrt RO_b, MW
SFs – 20%	134.4	141.12	127.68
MFs – 40%	268.8	282.24	255.36
Biz. – 20%	134.4	141.12	127.68
Agr. – 20%	134.4	141.12	127.68
totals (RO) – 100%	672.0	705.60	638.40

4 Case study data and its preprocessing

4.1 Data description

Raw consumer usage data for our empirical study was obtained from the Green Button project and PG&E [2]. The data was augmented to fill in missing values through interpolation/extrapolation and to represent the data on 15 min intervals. The original data represented power consumption on a 1 h interval basis. The power usage data spans a full year, starting from 12 AM 1st January through 11:45 PM 31st December. The data is organised into 15 min time intervals, so there are a total of 35,040 ($4 \times 24 \times 365$) rows of data. Each row of the data contains a power consumption reading (and the corresponding temperature reading) for the different CT's in *coastal*, *mountainous*, *inland*, and *desert* regions; each region consists of two types of SF and MF residential dwelling consumers. Additionally, it is assumed that this geographical area contains two types of business (of various sizes) and agricultural units and their corresponding temperature readings. Considering the preceding, there are ten different CTs and their corresponding ten temperature readings. It is assumed that this geographical area serves the needs of 1200 households for SF and 1200 MF households in each of the four regions and 60 businesses and 60 agricultural units for the entire geographical area. The coefficients of 1200 and 60 are conveniently selected for simulation purposes in order to make the total consumed power over the geographical area to hover around the threshold on 15 min intervals.

4.2 Simulated power distribution in IEEE 9-bus for active loads

The case study was created based on the IEEE 9-bus test system [15]. Scenario load flows were executed using the Power World simulation software [16]. After a study conducted through a series of load flow executions, which concentrates on loads 5, 6, and 8, as they are where the utility customer base to undergo demand pricing resides. The maximum deliverable power was set to 840 MW. Only active power was considered in this paper. The power usage threshold value is set to 672 MW (80% of the maximum deliverable power). For this case study, we are assuming that the utility companies offer discounted power usage pricing for staying below 672 MW and higher pricing above 672 MW. The threshold value is used as a target value to indicate whether power usage has exceeded its tolerable usage. Table 2 contains the power distribution per bus line (load) per consumer category (e.g. SF). For this case study, it is assumed that the different power consumer categories (e.g. SF) consume the same percentage of the total power in all the four geographical regions for computational convenience.

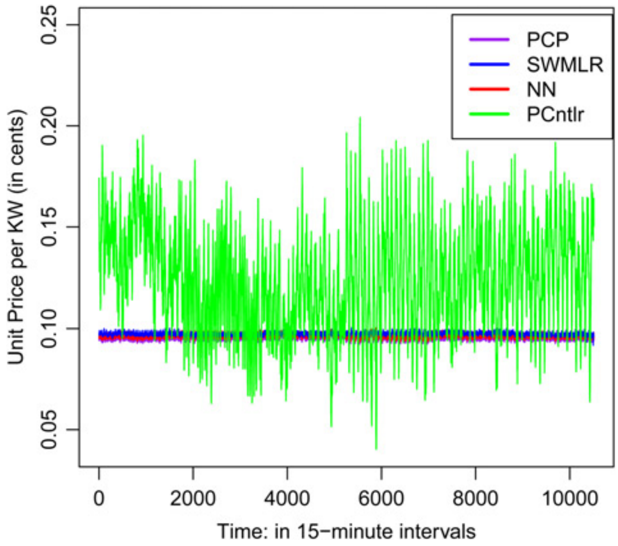

Fig. 3 *Results from the averaged computed unit prices (in cents) per kW using PCP, NNs, SWMLR, and PCntlr. PCP, shown in purple, is the benchmarked trend against which the other three models are compared. As shown, NNs' trend exhibits more accuracy, by staying close to PCP's trend, and stability with fewer fluctuations. Despite the sporadic overlaps in trends, the non-overlapping indicate statistical difference in unit price computations*

Analysis of Variance Table
Response: y
Df Sum Sq Mean Sq F value Pr(>F)
group 3 5.8030 1.93435 11696 < 2.2e-16 ***
Residuals 42044 6.9533 0.00017
—
Signif. codes: 0 *** 0.001 ** 0.01 * 0.05 . 0.1 1

Fig. 4 *Analysis of variance (ANOVA) of averages corresponding to Fig. 3*

4.3 PCP example

Table 3 contains a sample of consumed power consumption data for different residential CTs (**C**oastal, **M**ountainous, **I**nland, **D**esert,) and businesses – **Biz**, and agricultural units – **Agr**. Furthermore, residential types are shown in subcategories of SF and MF. For example, coastal single family (CSF) and coastal multi family

Table 4 Computed PCD using the sample data in Table 3

	EL (SFs)	EL (MFs)	EL (Biz.)	EL (Agr.)	RO (Adj.), MW	IM, MW	ND, MW	PCD, MW
RO_b	0.00	0.00	0.00	0.00	0.00	0.00	672	672
5% inc.	−3.60	−2.73	−9.00	−18.00	−7.39	−5211	706	672
5% dec.	2.40	1.82	6.00	12.00	4.92	31432	638	672

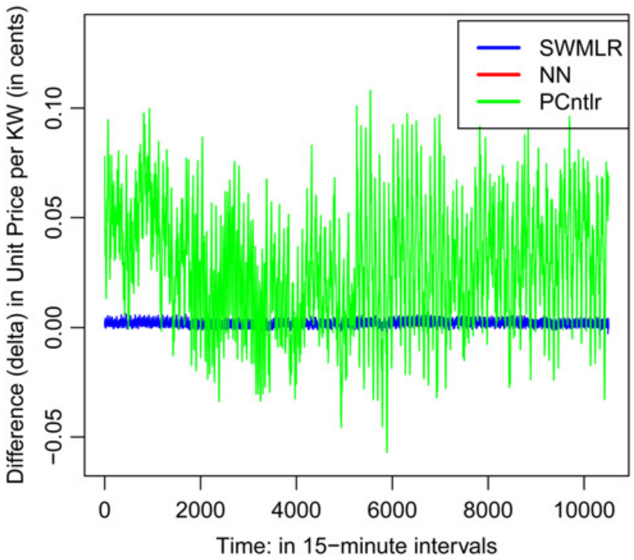

Fig. 5 *Results from taking the differences (deltas) of the averaged computed unit prices (in cents) per kW for NNs, SWMLR, and PCntlr against the PCP. In this figure, the X-axis (indicating the 15 min intervals for the year) also represents the normalised PCP trend*

Analysis of Variance Table
Response: y
Df Sum Sq Mean Sq F value Pr(>F)
group 2 4.9471 2.47354 10767 < 2.2e-16 ***
Residuals 31533 7.2440 0.00023
—
Signif. codes: 0 *** 0.001 ** 0.01 * 0.05 . 0.1   1

Fig. 6 *ANOVA of deltas corresponding to Fig. 5*

(CMF) represent SF and MF power consumptions in a coastal area, respectively etc. The percentages in 'Threshold (Base)' represent ratios of consumed power for each and every CT with respect to total consumed power for a given time interval – RO. The RO_b in column 'Threshold (Base)' is set at threshold value of 672 MW for the base price (b_p) of 10 cents per kW. Table 3 also demonstrates the consumed power increase/decrease (fluctuations) corresponding to increase/decrease in unit price per kW of 13 and 8 cents, respectively. Also, we assume elasticities of 0.25, 0.33, 0.01, and 0.05 for *all* SFs, *all* MFs, businesses, and agricultural units, respectively. The goal is to demonstrate that PCD for each and every 15 min interval (PCD_i) (see Section 3) remains constant despite the unit price (PCP) fluctuations. Table 4 contains the result of computations leading to determine the PCD, using (4)–(9) in Section 3.

4.4 Preprocessing

First, the data is processed to create the PCP data (see Section 3) as a basis of comparison against the data prediction models. This PCP is computed on a post-processed basis with full knowledge of consumer demands and elasticities. Second, *boosting* is used to create more datasets based on the original 35,040-row dataset in order to alleviate biasing while processing. In this process, the data is logically broken into 20 equal (logical) segments; various datasets are randomly selected for both *training* and *testing* for the NNs, and PCntlr models (PCntlr only requires testing sets and not training sets – see Section III-D-1). The training datasets contain one data segment (1752 rows) from the original dataset, whereas each testing dataset contains six segments (10,512 rows). NNs and the PCntlr are given the same testing datasets to ensure fairness. Please note that the PCntlr does not require training before it can operate on the test data and so the training step is skipped in that case. About 100 case study datasets, each comprised of six training and one testing datasets, were generated and used in order to achieve statistically significant results. In the case of NN's, training and testing datasets were executed using the NN Toolbox in MATLAB [17]. PCntlr's testing dataset *does not* require use of training dataset. The PCntlr algorithm (see Section 3.3) is run to compute the prices. The PCntlr was implemented using Microsoft Excel based on the formulation presented in Section 4.2. The preceding algorithms were repeated for NNs' and PCntlr over each of the 100 datasets. SWMLR receives 1 month of 15 min interval training data (a set of explanatory and their corresponding observed values – 4 × 24 × 30) based on the output of PCntlr. For that time period SWMLR builds fitting models (4 × 24) for each 15 min interval. Each fitting model is constructed using a month (30

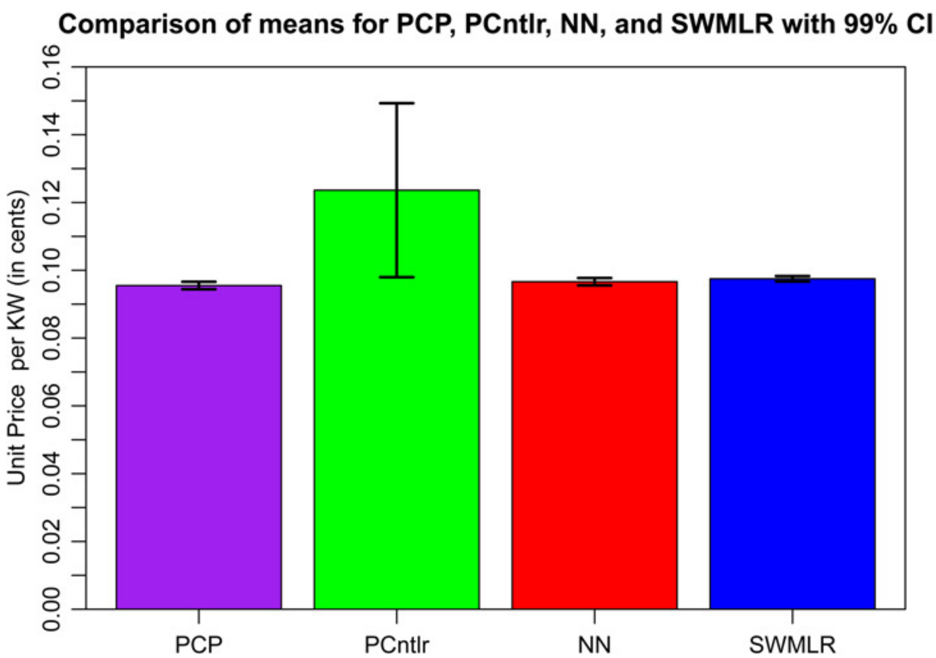

Fig. 7 *This figure is a different graphical representation of Fig. 3. As evident from this figure and Fig. 5, the NNs and SWMLR have nearly the same means. However, SWMLR exhibits less accuracy due to more fluctuation. The results are obtained with 99% confidence interval*

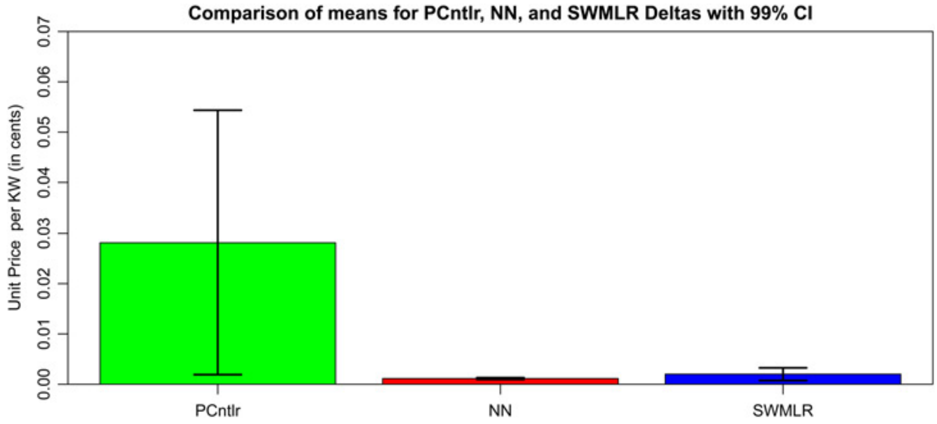

Fig. 8 *Analogous to Figs. 3 and 7, this figure is paired with Fig. 5 as an alternate way of depicting the differences (deltas) among NNs', SWMLR's, and PCntlr's trends in reference to PCP. Note that the X-axis also represents the normalised PCP. As evident, this figure indicates both the (relative) accuracy and stability of NNs in comparison with SWMLR and PCntlr. The results are obtained with 99% confidence interval*

Table 5 Advantages and disadvantages of NNs, SWMLR, and PCntlr approaches

NNs		SWMLR		PCntlr	
Adv.	DisAdv.	Adv.	DisAdv.	Adv.	DisAdv.
consistency (stability) of results	training time overhead. re-training with data change	non-linear behaviour simulation with linear segments	construction of fitting models requires borrowing observed values from PCntlr	simplicity of model's behaviour	coarse (relatively inaccurate) results due to linearity

days) of data. Fig. 2 depicts the data structure of SWMLR and the way it populates the predicted values. After filling in the predicted values for all the fitting models, we construct testing sets by first boosting the data (by creating 100 testing sets) followed by taking the average of those 100 sets.

5 Results' comparisons and analysis

In Figs. 3–8, the labels of *PCP*, *NN*, *SWMLR*, and *PCntlr* represent the (perfect) Price Controller, NNs, SWMLR, and the PCntlr, respectively. Fig. 3, and its companion ANOVA in Fig. 4, graphically indicate greater behavioural stability for NNs in comparison with SWMLR due to additional fluctuations present in the SWMLR results. Despite of nearly equal performance between NNs and SWMLR, SWMLR suffers from the disadvantage in that it relies on set of initial observed values (unit prices) obtained from PCntlr before it could construct the fitting models. This implies that SWMLR has a tight dependency on PCntlr and *must* run after running PCntlr. This may or may not be an issue depending on number of dependent and observed values and overall number of records. This is also evident in the bar plots depicted in Fig. 7 where, despite the nearly equal averages for NNs' and SWMLR, SWMLR exhibits more fluctuation in comparison with the NNs. Though the PCntlr's behavioural trend in Fig. 3 sporadically overlaps with NNs' and SWMLR's trends, PCntlr nonetheless has the worst performance of the three models due to its linearity (coarse approximation). This trend is also evident in computing the differences, in terms of deltas, between these three models with respect to the ideal perfect price controller; namely, PCntlr's performance consistently suffers in relation to NNs and SWMLR, as shown in Fig. 5 and its associated ANOVA in Fig. 6. The 99% confidence intervals for averages and deltas in Figs. 7 and 8 confirm the preceding observations. Table 5 contains the summary of the advantages and disadvantages of each model. Overall, NNs exhibit a superior performance in relation to the other two models. The disadvantage of NNs could be remedied with assigning a dedicated and powerful server in the presence of frequent data changes.

6 Conclusion

In this paper, we conducted an empirical comparison between non-linear, quasi-non-linear, and linear models represented by NNs, SWMLR, and PCntlr in the context of an energy DR system (DRMS). We used data derived from the Green Button Project and PG&E to create a case study where we could compare these approaches against a PCP, also referred to as the PCP model, as an empirical benchmark in order to determine the most efficient and appropriate approach for use in a DRMS. The datasets that we obtained were used as the basis for a mock scenario where different types of electricity consumers with different levels of price elasticity were modelled. Simulations were run using a combination of MATLAB, Excel, and R software platforms coupled with load flow results using Power World software application. The simulations allowed us to see the impact of price changes derived from the competing NNs, SWMLR, and PCntlr methods on net electricity demands. Our analysis found that the NNs approach was most suitable to DRMS due to its relative behavioural stability (consistency) in comparison with the other approaches for this dataset albeit that SWMLR looks promising as well. The future works entail expanding the comparison works by selecting additional different representative models and/or different datasets.

7 Acknowledgments

The views expressed in this document are those of the authors and do not reflect the official policy or position of the United Stated Air Force, Department of Defense, or the U.S. Government.

8 References

[1] Goel L., Wu Q., Wang P., *ET AL.*: 'Reliability enhancement of deregulated power systems considering demand-price elasticity'. Power

Engineering Conf., 2005. IPEC 2005. The Seventh Int., 2005, vol. 2, pp. 934–938
[2] 'Green Button Project Team'. Available at http://www.greenbuttondata.org/, accessed 20 February 2015
[3] Ozturk Y., Senthikumar D., Kumar S., ET AL.: 'An intelligent home energy management system to improve demand response', *IEEE Trans. Smart Grid*, 2012, **2**, (4), pp. 694–701
[4] Samadi P., Mohsenian-Rad A.-H., Schober R., ET AL.: 'Optimal real-time pricing algorithm based on utility maximization for smart grid'. 2010 First IEEE Int. Conf. on Smart Grid Communications (SmartGridComm), 2010, pp. 415–420
[5] Roos J.G., Lane I.E.: 'Industrial power demand response analysis for one-part real-time pricing', *IEEE Trans. Power Syst.*, 1998, **1**, (13), pp. 159–164
[6] Aalami H., Yousefi G.R., Moghadam M.P.: 'Demand response model considering EDRP and TOU programs', Transmission and Distribution Conf. and Exposition, 2008. T&D, 2008, pp. 1–6
[7] Su C.L., Kirschen D.: 'Quantifying the effect of demand response on electricity markets', *IEEE Trans. Power Syst.*, 2009, **3**, (24), pp. 1199–1207
[8] Xie L., Joo J.Y., Ilic M.D.: 'Integration of intermittent resources with price-responsive loads'. North American Power Symp. (NAPS), 2009, 2009, pp. 1–6
[9] Li N., Chen L., Low S.H.: 'Optimal demand response based on utility maximization in power networks'. 2011 IEEE Power and Energy Society General Meeting, 2011, pp. 1–8
[10] Keogh E., Chu S., Hart D., ET AL.: 'An online algorithm for segmenting time series'. Proc. IEEE Int. Conf. on Data Mining, 2001. ICDM 2001, 2001, pp. 289–296
[11] Minorsky N.: 'Directional stability of automatically steered bodies', *J. Am. Soc. Naval Eng.*, 1922, **2**, (34), pp. 280–309
[12] Liptak B.: 'Process control, Instrument engineer's handbook' (Chilton Book Company, Pennsylvania, USA, 1995), **1**, (34), pp. 20–29
[13] Bishop C.M.: 'Pattern recognition and machine learning' (Springer, New York, NY, USA, 2009)
[14] Witten I.H., Frank E., Hall M.A.: 'Data mining – practical machine learning tools and techniques' (Morgan Kaufmann, Burlington, MA, USA, 2011, 3rd edn.)
[15] 'IEEE – IEEE 9 Bus Test System'. Available at http://www.gobookee.org/ieee-9-bus-test-system-data, accessed 20 February 2015
[16] PowerWorld Corporation: 'PowerWorld corporation' (PowerWorld Corporation, Champaign, IL, USA, 2014)
[17] MATLAB: 'Version 7.13.0.564 (R2011b)' (The MathWorks Inc., Natick, MA, USA, 2011)